

## Pattern formation in the FitzHugh–Nagumo model



Qianqian Zheng <sup>a,b</sup>, Jianwei Shen <sup>a,\*</sup>

<sup>a</sup> Institute of Applied Mathematics, Xuchang University, Xuchang, Henan 461000, PR China

<sup>b</sup> School of Mathematics and Statistics, Zhengzhou University, Zhengzhou 450000, PR China

### ARTICLE INFO

#### Article history:

Received 21 April 2014

Received in revised form 25 April 2015

Accepted 27 June 2015

Available online 26 July 2015

#### Keywords:

Pattern formation  
FitzHugh–Nagumo model  
Turing–Hopf bifurcation  
Amplitude equation  
Secondary bifurcation  
Stability analysis

### ABSTRACT

In this paper, we investigate the effect of diffusion on pattern formation in FitzHugh–Nagumo model. Through the linear stability analysis of local equilibrium we obtain the condition how the Turing bifurcation, Hopf bifurcation and the oscillatory instability boundaries arise. By using the method of the weak nonlinear multiple scales analysis and Taylor series expansion, we derive the amplitude equations of the stationary patterns. The analysis of amplitude equations shows the occurrence of different complex phenomena, including Turing instability Eckhaus instability and zigzag instability. In addition, we apply this analysis to FitzHugh–Nagumo model and find that this model has very rich dynamical behaviors, such as spotted, stripe and hexagon patterns. Finally, the numerical simulation shows that the analytical results agree with numerical simulation.

© 2015 Elsevier Ltd. All rights reserved.

### 1. Introduction

FitzHugh–Nagumo model is a famous reaction–diffusion system which first introduced by Hodgkin and Huxley for the conduction of electrical impulses along a nerve fiber. Some mathematical models for biological neurons which represent neuronal behavior in terms of membrane potentials have been developed such as Hodgkin–Huxley model (1952), FitzHugh model (1969), Morris–Lecar model (1981), Hindmarsh–Rose model (1984), especially Hodgkin–Huxley model which is the motivation for the FitzHugh–Nagumo equation that extracts the essential behavior in a simple form [1–3]. A. Yazdan, G. Mehrdad and M. Ghasem have used the cellular automata method to simulate the pattern formation of FitzHugh–Nagumo model and considered the effects of different parameters of the FitzHugh–Nagumo model on changing the initial pattern [4]. A. Panfilov and P. Hogeweg found that the spiral breakup occurred spontaneously in the excitable media which have a shortened relative refractory period and is complicated [5]. The traveling waves, bifurcation and limit cycle of FitzHugh–Nagumo model (or modified) have been well studied [6–9]. The entrainment and modulation of time-evolutional patterns are not only investigated numerically in one dimension [10], but also Lee and Cho [11] find that the shape and type of Turing patterns depend on dynamical parameters and external periodic forcing. Moreover, Pena and Perez [12] show that slightly squeezed hexagons are locally stable in a full range of distortion angles. As we all know that the domain coarsening process is strongly affected by the spatial separation between groups created by the Turing pattern formation process [13] and further investigate the robustness problem [14,15]. Several groups have proposed possible candidates generating patterns since the dynamics of spontaneous pattern formation was first introduced to biology by Turing [16–18], and try to understand Biological Pattern Formation [19–22].

As we all can see, Amplitude equation is an important tool to investigate the react-diffusion system [23] and the focus of the investigation of pattern dynamics. However, the amplitude equation is a lengthy process, and only some systems

\* Corresponding author.

E-mail address: [xcjwshen@gmail.com](mailto:xcjwshen@gmail.com) (J. Shen).

have been chosen in the past for amplitude equation [24]. In this paper, we would make research on pattern selection of FitzHugh–Nagumo model (FN model) by using the standard multiple scale analysis [25,26]. As we know that the effect of space on FN model was not taken into account in the previous works or some results were obtained by choosing particular initial conditions [27]. Especially the reaction term of fractional order is never considered and do not have a formal way to solve it [28–31].

Eckhaus and zigzag instability which is rarely studied is ubiquitous secondary bifurcation [28,32]. We know that the Turing instability leads to small amplitude stationary periodic patterns, and affect the stability of the pattern formation by secondary instabilities, such as Eckhaus and zigzag which may act in a coupled way. In addition, they can also cause large amplitude periodic patterns. The amplitude equation has been used to study secondary instabilities which took the form of a NWS equation about some models [33], and some meaningful results, which is important to explain biological phenomenon, was obtain.

In order to understand further the conduction of electrical impulses along a nerve fiber, we plan to model this network with mathematical model. It is well known that the reaction–diffusion system is quite ubiquitous in nature, so we also investigate the relationship between the reaction–diffusion system and the conduction of electrical impulses along a nerve fiber. As we know that the diffusion is often caused by intensity of pressure and density, and the diffusion can sometimes destabilize the stable equilibrium. If the parameter reach a threshold value, the system will emerge the Hopf bifurcation or Turing bifurcation. In nature, the Turing pattern which can induce the complex behaviors often occurs in physiological regulatory systems with diffusion.

In recent years, many scientists deemed that mathematical modeling could be used to investigate the differences at the dynamical level between healthy and pathologic configurations of biological pathways [23,34–36]. By using the mathematical model, the researchers detected the key points regulating main properties of biological system and find the methods to solve the different diseases. However, they only studied periodic oscillation, delay, linear stability analysis and some theoretical introduction about pattern formation for this model. In addition, we will give the condition of Turing bifurcation, derive the amplitude equation, and study the Eckhaus instability and zigzag instability by taking the form of NWS equation.

In this paper, we will investigate the dynamics of the conduction of electrical impulses along a nerve fiber, and reveal how the dynamics of ion conduction is affected by diffusion. In Section 2, we give the model represented by mathematical model and some theoretical results. In Section 3, we give the stability analysis of Hopf and Turing bifurcation. In Section 4, we derive the amplitude equation from react-diffusion system. In Section 5, we analyze the stability of pattern formation and pattern selection by using the amplitude equation. In Section 6, we studied the stability of NWS which was derived from amplitude equation. In Section 7, we show the numerical analysis of the network. Finally, we summarize our results.

## 2. The model

As we all know that ionic diffusion is ubiquitous when ion passes through the cytomembrane, so we should consider the effect of diffusion on the system. In this paper, we add the diffusion to the system, and obtain the reaction-diffusing system as follows.

$$\begin{cases} \frac{\partial u}{\partial t} = (a - u)(u - 1)u - v + D_1 \Delta u \\ \frac{\partial v}{\partial t} = e(bu - v) + D_2 \Delta v \end{cases} \quad (2.1)$$

where  $\Delta = \frac{\partial^2}{\partial x^2} + \frac{\partial^2}{\partial y^2}$  is the laplace operator and  $(x, y) \in R^2$ . The meaning of the variables and parameters are different from the original FitzHugh–Nagumo model, which was introduced in [37]. In the model,  $u$  represents the membrane potential.  $v$  represents the recovery variable,  $a$  represents the excitatory threshold,  $e$  represents the excitability and  $b, e$  are parameters that can change the rest state and dynamics.

## 3. Linear stability analysis of system (2.1)

In this section we perform a linear stability analysis for the reaction–diffusion system (2.1), and derive a set of conditions for pattern formation. We assume the steady state solution of Eq. (2.1) is at  $(p_0, m_0)$ . Although the system is a nonlinear system, linear steady analysis is applied to the system (2.1) when it lies in onset of the bifurcation point. For the stability of this spatially uniform solution we consider a perturbation of the form

$$U(t) = \begin{pmatrix} u(t) \\ v(t) \end{pmatrix} = \begin{pmatrix} u(t) - u_0 \\ v(t) - v_0 \end{pmatrix}$$

where  $(u_0, v_0) = (\frac{1+a+\sqrt{(1-a)^2-4b}}{2}, bu_0)$ .

The linearized system governing the dynamics of  $U$  is defined by

$$U_t = CU + D\Delta U \quad (3.1)$$

where the coefficient matrix is given by

$$C = \begin{pmatrix} m_{11} & m_{12} \\ m_{21} & m_{22} \end{pmatrix}, \quad D = \begin{pmatrix} D_1 & 0 \\ 0 & D_2 \end{pmatrix}$$

where

$$m_{11} = 2a + 3b - (a+1) \frac{1+a+\sqrt{(1-a)^2-4b}}{2}, \quad m_{12} = -1, \quad m_{22} = be, \quad m_{21} = -e.$$

In the standard way, we assume that  $u$  takes the form

$$U = \begin{pmatrix} c_1 \\ c_2 \end{pmatrix} e^{\lambda t + ikr}$$

and get the characteristic equation from the system (3.1) as follows.

$$\begin{vmatrix} \lambda - m_{11} + k^2 D_1 & -m_{12} \\ -m_{21} & \lambda - m_{22} + k^2 D_2 \end{vmatrix} = 0.$$

In final, we solve the characteristic equation and obtain the eigenvalues

$$\begin{aligned} \lambda_k^2 - Tr_k \lambda + \delta(k^2) &= 0 \\ \lambda_k &= \frac{1}{2}(Tr_k \pm \sqrt{Tr_k^2 - 4\delta_k}) \end{aligned} \tag{3.2}$$

where

$$\begin{aligned} Tr_k &= m_{11} + m_{22} - k^2(D_1 + D_2), \quad Tr_0 = m_{11} + m_{22} \\ \delta(k^2) &= m_{11}m_{22} - m_{12}m_{21} - (m_{11}D_2 + m_{22}D_1)k^2 + D_1D_2k^4 \\ \det(C) &= \delta_0 = m_{11}m_{22} - m_{12}m_{21}. \end{aligned}$$

**Lemma 1.** If  $\text{Im}(\lambda_k) \neq 0$ ,  $\frac{\partial \Re(\lambda_k)}{\partial \mu} \neq 0$  and  $\text{Re}(\lambda_k) = 0$  when  $k = 0$ , the Hopf bifurcation occurs, and the Turing bifurcation (diffusion-driven instability) occurs in the reaction-diffusion system which should satisfy the following conditions here.

- (i)  $Tr_0 = m_{11} + m_{22} < 0$
- (ii)  $\det(C) = \delta_0 = m_{11}m_{22} - m_{12}m_{21} > 0$
- (iii)  $m_{11}D_2 + m_{22}D_1 > 0$
- (iv)  $m_{11}D_2 + m_{22}D_1 > 2\sqrt{D_1D_2(m_{11}m_{22} - m_{12}m_{21})}$ .

The critical condition is  $\text{Im}(\lambda_k) = 0$  and  $\text{Re}(\lambda_k) = 0$  when  $k \neq 0$ .

**Lemma 2** (The Intermediate Value Theorem of Continuous Functions). Consider the polynomial  $p(x) = x^{2n} + a_1x^{2n-1} + \dots + a_{2n} = 0$ , ( $n = 1, 2, \dots$ ), if  $a_{2n} < 0$ , then  $p(x)$  has at least one positive root.

**Proof.** Assume  $x_i$  ( $i = 1, 2, \dots, 2n$ ) is the roots of  $p(x)$  and  $x_i$  have two cases: Real root, Imaginary root. As we know the number of imaginary root is even, then their product is positive. Now we just consider the real root. Obviously, the number of real root is even, if all real roots are negative, then their product is positive. However,  $a_{2n} = \prod_{i=1}^{2n} x_i < 0$ , clearly, there exists contradiction. So there is at least one positive root. The proof is completed.

Here we assume that

$$d = \frac{D_2}{D_1}.$$

**Theorem 1.** Based on lemma, we can get the following conclusion:

- (i) If  $e = 2a + 3b - (a+1) \frac{1+a+\sqrt{(1-a)^2-4b}}{2}$ , then the Hopf bifurcation of the system (2.1) without diffusion occurs.
- (ii) If  $(2a + 3b - (a+1) \frac{1+a+\sqrt{(1-a)^2-4b}}{2} + de)^2 - 4dbe = 0$ , then the Turing bifurcation of the system (2.1) occurs.
- (iii) Assuming that  $\delta(k^2) < 0$  for some  $k^2 \neq 0$ , we can achieve a diffusion-driven instability and also get the minimum value of  $\delta_k$  about  $k^2$  to be negative, and get critical value  $k_c^2 = \frac{m_{11}D_2 + m_{22}D_1}{2D_1D_2}$ .

The proof of Lemma 1 and Theorem 1 can be obtained easily by using the theorem in [24], we ignore it here.

#### 4. The amplitude equation of system (2.1)

As we know that the amplitude of Eq. (2.1) cannot be directly deduced, therefore we expand Eq. (2.1) at equilibrium  $(u_0, v_0)$  by using the Taylor expansion and then we truncate the expansion at third order as follows.

$$\begin{aligned}\frac{\partial u}{\partial t} &= (a - u)(u - 1)u - v + D_1 \Delta u \\ \frac{\partial v}{\partial t} &= e(bu - v) + D_2 \Delta v.\end{aligned}\quad (4.1)$$

In the following, we use multiple scale analysis to derive the amplitude equations when  $|k| = k_c$ . Denote  $\gamma$  as the controlled parameters. When the controlled parameter is larger than the critical value of Turing point, the solutions of systems (4.1) can be expanded as

$$c = c_0 + \sum_{i=1}^N (Z_i e^{ik_i r})$$

with  $|k| = k_c$ ,  $Z_j$  and the conjugate  $\bar{Z}_j$  are the amplitudes associated with the modes  $k_j$  and  $-k_j$ .

Close to onset  $\gamma = \gamma_c$ , one has that  $\frac{\partial Z_i}{\partial t} = s_i Z_i + F_i(Z_i, Z_j, \dots)$ .

Based on the center manifold near the Turing bifurcation point, it can be concluded that amplitude  $Z_j$  satisfies  $\frac{\partial Z_i}{\partial t} = F_i(Z_i, \bar{Z}_j, Z_j, \bar{Z}_j, \dots)$ .

From the standard multiple scale analysis, up to the third order in the perturbations, the spatiotemporal evolution of the amplitudes can be described as

$$\tau_0 \frac{\partial Z_i}{\partial t} = \mu Z_i + \sum_{lm} h_{lm} Z_l Z_m + \sum_{lm} g_{lmn} Z_l Z_m Z_n. \quad (4.2)$$

Due to spatial translational symmetry, we have the following equation:

$$\tau_0 \frac{\partial Z_i}{\partial t} e^{ik_i r} = \mu Z_i e^{ik_i r} + \sum_{lm} h_{lm} Z_l Z_m e^{i(k_l + k_m)r} + \sum_{lm} g_{lmn} Z_l Z_m Z_n e^{i(k_l + k_m + k_n)r}. \quad (4.3)$$

Comparing (4.2) with (4.3), one can find that the two equations hold only if  $k_i = k_l + \dots + k_m$ . From the center manifold theory, we know that amplitude equations do not include the amplitude with unstable mode. As a result, we have the following equations:

$$\begin{aligned}\tau_0 \frac{\partial Z_1}{\partial t} &= \mu Z_1 + h \bar{Z}_2 \bar{Z}_3 - (g_1 |Z_1|^2 + g_2 |Z_2|^2 + g_3 |Z_3|^2) Z_1 \\ \tau_0 \frac{\partial Z_2}{\partial t} &= \mu Z_2 + h \bar{Z}_1 \bar{Z}_3 - (g_1 |Z_2|^2 + g_2 |Z_3|^2 + g_3 |Z_1|^2) Z_2 \\ \tau_0 \frac{\partial Z_3}{\partial t} &= \mu Z_3 + h \bar{Z}_2 \bar{Z}_1 - (g_1 |Z_3|^2 + g_2 |Z_1|^2 + g_3 |Z_2|^2) Z_3\end{aligned}$$

where  $\mu = \frac{e - e_c}{e_c}$  and  $\tau_0$  is constant. The another case we can get by changing subscript which are not described in detail here.

In the following, we will give the expressions of  $\tau_0$ ,  $h$ ,  $g_1$ ,  $g_2$ . Let the system (4.1) be written as

$$\frac{\partial c}{\partial t} = Lc + N(c, c)$$

where

$$c = \begin{pmatrix} u \\ v \end{pmatrix}$$

is the variables

$$L = \begin{pmatrix} -a + D_1 \nabla^2 & -1 \\ be & -e + D_2 \nabla^2 \end{pmatrix}$$

is the linear operator

$$N = \begin{pmatrix} (a + 1)u^2 - u^3 \\ 0 \end{pmatrix}$$

is the nonlinear term.

We need to investigate the dynamical behavior when  $\gamma$  is close to  $\gamma_c$ , and then we expand  $\gamma$  as

$$e_c - e = \varepsilon e_1 + \varepsilon^2 e_2 + \dots$$

where  $\varepsilon$  is a small enough parameter. We expand  $U$  and  $N$  as the series form of  $\varepsilon$ :

$$\begin{aligned} U &= \begin{pmatrix} u \\ v \end{pmatrix} = \begin{pmatrix} u_1 \\ v_1 \end{pmatrix} \varepsilon + \begin{pmatrix} u_2 \\ v_2 \end{pmatrix} \varepsilon^2 + \dots \\ N &= \begin{pmatrix} (au_1^2 + u_1^2)\varepsilon^2 + ((a+1)u_1u_2 + u_1^3)\varepsilon^3 + o(\varepsilon^4) \\ 0 \end{pmatrix}. \end{aligned}$$

Linear operator  $L$  can be expanded as

$$L = L_c + (e_c - e)M \quad (4.4)$$

where

$$L_c = \begin{pmatrix} -a + D_1 \nabla^2 & -1 \\ b e_c & e_c + D_2 \nabla^2 \end{pmatrix}, \quad M = \begin{pmatrix} 0 & 0 \\ -b & -1 \end{pmatrix}.$$

Let

$$T_0 = t, \quad T_1 = \varepsilon t, \quad T_2 = \varepsilon^2 t \dots$$

and  $T_i$  is a dependent variable. For the derivation of time, we have that

$$\frac{\partial}{\partial t} = \frac{\partial}{\partial T_0} + \varepsilon \frac{\partial}{\partial T_1} + \varepsilon^2 \frac{\partial}{\partial T_2} + \dots$$

The solutions of systems (3.1) have the following form:

$$C = \begin{pmatrix} u \\ v \end{pmatrix} = \sum_{i=1}^3 \begin{pmatrix} x_i \\ y_i \end{pmatrix} e^{ik_i r}.$$

This expression implies that the bases of the solutions have nothing to do with time and the amplitude  $Z$  is a variable that changes slowly. As a result, one has the following equation:

$$\frac{\partial Z}{\partial t} = \varepsilon \frac{\partial Z}{\partial T_1} + \varepsilon^2 \frac{\partial Z}{\partial T_2} + \dots \quad (4.5)$$

Substituting the above equations into (4.4) and expanding (4.4) according to different orders of  $\varepsilon$ , we can obtain three equations as follows:

$$\begin{aligned} \varepsilon : L_c \begin{pmatrix} u_1 \\ v_1 \end{pmatrix} &= 0 \\ \varepsilon^2 : L_c \begin{pmatrix} u_2 \\ v_2 \end{pmatrix} &= \frac{\partial}{\partial T_1} \begin{pmatrix} u_1 \\ v_1 \end{pmatrix} - e_1 M \begin{pmatrix} u_1 \\ v_1 \end{pmatrix} - \begin{pmatrix} (a+1)u_1^2 \\ 0 \end{pmatrix} \\ \varepsilon^3 : L_c \begin{pmatrix} u_3 \\ v_3 \end{pmatrix} &= \frac{\partial}{\partial T_1} \begin{pmatrix} u_2 \\ v_2 \end{pmatrix} + \frac{\partial}{\partial T_2} \begin{pmatrix} u_1 \\ v_1 \end{pmatrix} - e_1 M \begin{pmatrix} u_2 \\ v_2 \end{pmatrix} - e_2 M \begin{pmatrix} u_1 \\ v_1 \end{pmatrix} \begin{pmatrix} (a+1)u_1v_1 - u_1^3 \\ 0 \end{pmatrix}. \end{aligned}$$

We first consider the case of the first order of  $\varepsilon$ . Since  $L_c$  is the linear operator of the system close to the onset,  $(u_1, v_1)^T$  is the linear combination of the eigenvectors that corresponds to the eigenvalue zero. Since that

$$\begin{pmatrix} u \\ v \end{pmatrix} = \sum_{i=1}^3 \begin{pmatrix} x_i \\ y_i \end{pmatrix} e^{ik_i r} + \text{c.c.}$$

and can obtain that  $x_i = B y_i$ .

Let  $x_i = B$  by assuming  $y_i = 1$  then

$$\begin{pmatrix} u_1 \\ v_1 \end{pmatrix} = \begin{pmatrix} B \\ 1 \end{pmatrix} (W_1 e^{ik_1 r} + \text{c.c.}), \quad (i = 1, 2, 3)$$

where  $B = -\frac{1}{a+D_1 k^2}$ ,  $|k_i| = k_c$  and  $W_i$  is the amplitude of the mode  $e^{ik_i r}$ .

Now, we consider the case of  $\varepsilon^2$ . According to the Fredholm solubility condition, the vector function of the right hand of the above equation must be orthogonal with the zero eigenvectors of operator  $L_c^+$ . The zero eigenvectors of adjoint operator  $L_c^+$  are

$$\begin{pmatrix} 1 \\ A \end{pmatrix} e^{-ik_1 r}$$

where  $A = \frac{a+D_1 k^2}{b e_c}$ .

It can be found from the orthogonality condition that

$$(1 - A) e^{-ik_i r} L_c \begin{pmatrix} u_2 \\ v_2 \end{pmatrix} = 0.$$

It can be obtained from the orthogonality condition that

$$\frac{\partial}{\partial T_1} (u_1 + Av_1) + e_1 A (bu_1 + v_1) - (a+1)u_1^2.$$

By investigating  $e^{ik_1 r}$  only in the following, the another case we can get by changing subscript which are not described in detail here, one has

$$(A+B) \frac{\partial W_1}{\partial T_1} = -e_1 A (Bb+1) W_1 + B^2 (a+1) \overline{W_2 W_3}. \quad (4.6)$$

By using the same methods, one has

$$\begin{pmatrix} u_2 \\ v_2 \end{pmatrix} = \begin{pmatrix} a_0 \\ b_0 \end{pmatrix} + \begin{pmatrix} a_i \\ b_i \end{pmatrix} e^{ik_i r} + \begin{pmatrix} a_{ii} \\ b_{ii} \end{pmatrix} e^{i2k_i r} + \begin{pmatrix} a_{12} \\ b_{12} \end{pmatrix} e^{i(k_1-k_2)r} + \begin{pmatrix} a_{23} \\ b_{23} \end{pmatrix} e^{i(k_2-k_3)r} + \begin{pmatrix} a_{31} \\ b_{31} \end{pmatrix} e^{i(k_3-k_1)r} + \text{c.c.}$$

For the case of  $\varepsilon^3$ , we have that

$$\begin{aligned} (-a + D_1 \nabla^2) u_2 - v_2 &= \frac{\partial u_1}{\partial T_1} - (a+1)u_1^2 \\ be_c u_2 + (e_c + D_2 \nabla^2) v_2 &= \frac{\partial v_1}{\partial T_1} + e_1 (bu_1 + v_1) \end{aligned}$$

and we can get

$$\begin{aligned} b_0 &= -\frac{1}{b} E_1(|W_i|^2), \quad a_0 = E_1(|W_i|^2), \\ a_i &= Bb_i, \quad a_{ii} = E_3 W_i^2, \quad b_{ii} = \frac{be_c}{4D_2 k^2 - e_c}, \quad a_{12} = E_4 W_1 \overline{W_2}, \quad b_{12} = \frac{be_c}{3D_2 k^2 - e_c} E_4 W_1 \overline{W_2} \end{aligned}$$

where

$$E_1 = \frac{2B^2}{a-b}, \quad E_3 = \frac{B^2(a+1)(4D_2 k^2 - e_c)}{(a+4D_1 k^2)(4D_2 k^2 - e_c) + be_c}, \quad E_4 = \frac{B^2(a+1)(3D_2 k^2 - e_c)}{(a+3D_1 k^2)(3D_2 k^2 - e_c) + be_c}.$$

Using the Fredholm solubility condition again, we can obtain

$$\begin{aligned} (A+B) \left( \frac{\partial W_1}{\partial T_2} + \frac{\partial a_1}{\partial T_1} \right) &= -e_1 A (Bb+1) b_1 - e_2 A (Bb+1) W_1 - B(a+1)(E_1|W_i|^2) W_1 \\ &\quad + E_4 (|W_2| + |W_3|) W_1 + B^2 (a+1) (\overline{W_2 b_3} + \overline{W_3 b_2}) + 3B^2 (|W_i|) W_1. \end{aligned} \quad (4.7)$$

For simplification, we substitute the system (4.6) and (4.7) into (4.5), and obtain the following equation

$$\begin{aligned} (A+B) \frac{\partial Z_1}{\partial T} &= (e_c - e) Z_1 + B^2 (a+1) \overline{Z_2 Z_3} - ((E_1 B(a+1) - 3B^2) |Z_1|^2 \\ &\quad - (E_1 B(a+1) + E_4 - 3B^2) |Z_2|^2 + (E_1 B(a+1) + E_4 - 3B^2) |Z_3|^2) Z_1. \end{aligned}$$

By calculations, we obtain the expressions of the coefficients of  $\tau_0$ ,  $h$ ,  $g_1$ , and  $g_2$  as follows:  $\tau_0 = \frac{A+B}{e_c}$ ,  $h = \frac{B^2(a+1)}{e_c}$ ,  $g_1 = \frac{E_1 B(a+1) - 3B^2}{e_c}$ ,  $g_2 = \frac{E_1 B(a+1) + E_4 - 3B^2}{e_c}$ . So the equation of amplitude is as follows:

$$\begin{aligned} \tau_0 \frac{\partial Z_1}{\partial t} &= \mu Z_1 + h \overline{Z_2 Z_3} - (g_1 |Z_1|^2 + g_2 |Z_2|^2 + g_3 |Z_3|^2) Z_1 \\ \tau_0 \frac{\partial Z_2}{\partial t} &= \mu Z_2 + h \overline{Z_1 Z_3} - (g_1 |Z_2|^2 + g_2 |Z_1|^2 + g_3 |Z_3|^2) Z_2 \\ \tau_0 \frac{\partial Z_3}{\partial t} &= \mu Z_3 + h \overline{Z_1 Z_2} - (g_1 |Z_3|^2 + g_2 |Z_2|^2 + g_3 |Z_1|^2) Z_3. \end{aligned} \quad (4.8)$$

This is a so complex process to achieve the amplitude equation. In this section, we make use of the weak nonlinear multiple scales analysis and Taylor series expansion to obtain the amplitude equation, this process is very trivial detail and we only depend on the Maple soft and manpower calculation that few people would like to put much time in it. In the future, we hope we can find some program to solve it.

## 5. Linear stability analysis of the amplitude equation

In this section, we will investigate the dynamics of amplitude equation by using the linear stability analysis and study the different pattern. Firstly, we assume that the amplitude in (4.8) may be expressed as follows.

$$Z_i = \rho_i e^{i\phi_i} \quad (5.1)$$

where  $\rho_i = |Z_i|$  and  $\phi_i$  is the phase. We incorporate the system (5.1) into Eq. (4.8), then separate the real and imaginary parts. Finally, we obtain the equation as follows.

$$\begin{aligned} \tau_0 \frac{\partial \phi}{\partial t} &= -h \frac{\rho_1^2 \rho_2^2 + \rho_1^2 \rho_3^2 + \rho_3^2 \rho_2^2}{\rho_1 \rho_2 \rho_3} \sin(\phi) \\ \tau_0 \frac{\partial \rho_1}{\partial t} &= \mu \rho_1 + h \rho_2 \rho_3 \cos(\phi) - (g_1 |\rho_1|^2 + g_2 |\rho_2|^2 + g_3 |\rho_3|^2) \rho_1 \\ \tau_0 \frac{\partial \rho_2}{\partial t} &= \mu \rho_2 + h \rho_1 \rho_3 \cos(\phi) - (g_1 |\rho_2|^2 + g_2 |\rho_1|^2 + g_3 |\rho_3|^2) \rho_2 \\ \tau_0 \frac{\partial \rho_3}{\partial t} &= \mu \rho_3 + h \rho_2 \rho_1 \cos(\phi) - (g_1 |\rho_3|^2 + g_2 |\rho_2|^2 + g_3 |\rho_1|^2) \rho_3 \end{aligned} \quad (5.2)$$

where  $\phi = \phi_1 + \phi_2 + \phi_3$ . From the system (5.2), we can know that the phase of pattern amplitude only lies in the phase  $\phi = 0$  and  $\phi = \pi$  when the system lies the stationary state. Because of all the  $\rho_i \geq 0$ , we can know that the solution of  $\tau_0 \frac{\partial \phi}{\partial t} = -h \frac{\rho_1^2 \rho_2^2 + \rho_1^2 \rho_3^2 + \rho_3^2 \rho_2^2}{\rho_1 \rho_2 \rho_3} \sin(\phi)$  is stable for  $\phi = 0$  when  $h > 0$ , and the solution is stable for  $\phi = \pi$  when  $h < 0$ . If we only consider the stable solution of  $\tau_0 \frac{\partial \phi}{\partial t} = -h \frac{\rho_1^2 \rho_2^2 + \rho_1^2 \rho_3^2 + \rho_3^2 \rho_2^2}{\rho_1 \rho_2 \rho_3} \sin(\phi)$ , the mode equation have the form as follows:

$$\tau_0 \frac{\partial \rho_1}{\partial t} = \mu \rho_1 + |h| \rho_2 \rho_3 - (g_1 |\rho_1|^2 + g_2 |\rho_2|^2 + g_3 |\rho_3|^2) \rho_1. \quad (5.3)$$

The another equation we can be obtained by changing subscript which are not described in detail here.

The dynamical systems (5.3) possess four kinds of solution as follows. In order to investigate the pattern formation, we will execute the stability analysis on the four kinds of stationary solution, the stability of four kinds of stationary solution can be obtained by a linear stability analysis when we add the perturbation  $(\delta \rho_1, \delta \rho_2, \delta \rho_2)$  to  $(\rho_1, \rho_2, \rho_2)$ , substitute it in Eq. (5.3), and get rid of higher order term, we can obtain linear perturbation equation. The matrix of equation is mode equation have the form as follows:

$$\begin{pmatrix} \mu - 3g_1 \rho_1^2 - g_2 (\rho_2^2 + \rho_3^2) & |h| \rho_3 - 2g_2 \rho_2 \rho_1 & |h| \rho_2 - 2g_2 \rho_3 \rho_1 \\ |h| \rho_3 - 2g_2 \rho_2 \rho_1 & \mu - 3g_1 \rho_2^2 - g_2 (\rho_1^2 + \rho_3^2) & |h| \rho_1 - 2g_2 \rho_2 \rho_3 \\ |h| \rho_2 - 2g_2 \rho_3 \rho_1 & |h| \rho_1 - 2g_2 \rho_2 \rho_3 & \mu - 3g_1 \rho_3^2 - g_2 (\rho_1^2 + \rho_2^2) \end{pmatrix}. \quad (5.4)$$

(i) The stationary state  $\rho_1 = \rho_2 = \rho_3 = 0$ .

The stationary state corresponding to the linear perturbation equation is  $\frac{\partial \Delta \rho_i}{\partial t} = \mu \Delta \rho_i$  we can know easily that the stationary is stable when  $\mu < \mu_2 = 0$ , conversely it is unstable.

(ii) Stripe patterns  $\rho_1 = \sqrt{\frac{\mu}{g_1}}$ ,  $\rho_2 = \rho_3 = 0$ .

We substitute  $(\rho, 0, 0)$  in the perturbation equation (5.4), one obtains

$$\tau_0 \frac{d}{dt} \begin{pmatrix} \Delta \rho_1 \\ \Delta \rho_2 \\ \Delta \rho_3 \end{pmatrix} = \begin{pmatrix} \mu - 3g_1 \rho & 0 & 0 \\ 0 & \mu - g_2 \rho^2 & |h| \rho \\ 0 & |h| \rho & \mu - g_2 \rho \end{pmatrix} \begin{pmatrix} \Delta \rho_1 \\ \Delta \rho_2 \\ \Delta \rho_3 \end{pmatrix}. \quad (5.5)$$

For  $\rho_1 = \sqrt{\frac{\mu}{g_1}}$ , the eigenvalue of matrix of Eq. (5.5)  $\lambda_i$  is determined by the following characteristic equation:

$$(\lambda + 2\mu) \left( \left( \lambda - \mu + \frac{g_2}{g_1} \right) - \frac{h^2}{g_1} \mu \right) = 0$$

which has three eigenvalues is

$$\lambda_1 = -2\mu, \quad \lambda_{2,3} = \mu \left( 1 - \frac{g_2}{g_1} \pm |h| \sqrt{\frac{\mu}{g_1}} \right).$$

For  $\mu > 0$ ,  $\frac{g_2}{g_1} > 1$ , so the condition of all the eigenvalues which are negative is  $\mu > \mu_3 = h^2 \frac{g_1}{g_2 - g_1}$  and all the perturbation to stripe pattern will disappear with time.

(iii) Hexagon patterns  $\rho_1 = \rho_2 = \rho_3 = \frac{|h| \pm \sqrt{h^2 + 4(g_1 + 2g_2)\mu}}{2(g_1 + 2g_2)}$ .

For the hexagon patterns, we also substitute the stationary  $\rho = \rho_1 = \rho_2 = \rho_3 = \frac{|h| \pm \sqrt{h^2 + 4(g_1 + 2g_2)\mu}}{2(g_1 + 2g_2)}$  in the perturbation equation (5.4), one obtains

$$\tau_0 \frac{d}{dt} \begin{pmatrix} \Delta\rho_1 \\ \Delta\rho_2 \\ \Delta\rho_3 \end{pmatrix} = \begin{pmatrix} p & q & q \\ q & p & q \\ q & q & p \end{pmatrix} \begin{pmatrix} \Delta\rho_1 \\ \Delta\rho_2 \\ \Delta\rho_3 \end{pmatrix} \quad (5.6)$$

where  $p = \mu - (3g_1 + 2g_2)\rho^2$ ,  $q = |h|\rho - 2g_2\rho^2$ . The characteristic equation is

$$(p - \lambda)^3 - 3q^2(p - \lambda) + 2q^3 = 0$$

which has three eigenvalue is

$$\lambda_1 = \lambda_2 = -q + p, \quad \lambda_3 = 2q + p$$

substitute the stationary in it, and we always have  $\lambda_3 > 0$  for  $\rho^- = \frac{|h| - \sqrt{h^2 + 4(g_1 + 2g_2)\mu}}{2(g_1 + 2g_2)}$ , so the pattern is unstable. All the eigenvalues are negative for  $\rho^+ = \frac{|h| + \sqrt{h^2 + 4(g_1 + 2g_2)\mu}}{2(g_1 + 2g_2)}$  when  $\mu < \mu_4 = \frac{2g_1 + g_2}{(g_2 - g_1)^2}h^2$ , the pattern is stable.

(iv) The mixed states  $\rho_1 = \frac{|h|}{g_2 - g_1}$ ,  $\rho_2 = \rho_3 = \sqrt{\frac{\mu - g_1 h^2}{g_1 + g_2}}$ . By using the same methods we can obtain

$$\tau_0 \frac{d}{dt} \begin{pmatrix} \Delta\rho_1 \\ \Delta\rho_2 \\ \Delta\rho_3 \end{pmatrix} = \begin{pmatrix} p_1 & q_1 & q_1 \\ q_1 & p_2 & q_2 \\ q_1 & q_2 & p_2 \end{pmatrix} \begin{pmatrix} \Delta\rho_1 \\ \Delta\rho_2 \\ \Delta\rho_3 \end{pmatrix} \quad (5.7)$$

where

$$p_1 = \mu - 3g_1\rho_1^2 - g_2(\rho_2^2 + \rho_3^2) = \frac{g_1 - g_2}{g_1 + g_2}\mu - \frac{(3g_1 + g_2)g_1h^2}{(g_1 + g_2)(g_1 - g_2)^2}$$

$$p_2 = \mu - 3g_1\rho_2^2 - g_2(\rho_1^2 + \rho_3^2) = \frac{-2g_1}{g_1 + g_2}\mu + \frac{(3g_1^2 - g_2^2)g_1h^2}{(g_1 + g_2)(g_1 - g_2)^2}$$

$$q_1 = |h|\rho_2 - 2g_2\rho_2\rho_1 = \sqrt{\frac{g_1 + g_2}{(g_1 - g_2)^2} \left[ \mu - \frac{g_1h^2}{(g_1 - g_2)^2} \right]} |h|$$

$$q_2 = |h|\rho_1 - 2g_2\rho_2^2 = \frac{-2g_2}{g_1 + g_2}\mu + \frac{g_2^2 - g_1^2 + 2g_1g_2h^2}{(g_1 + g_2)(g_1 - g_2)^2}.$$

The characteristic equation is

$$[\lambda^2 - (p_1 + p_2 + p_3)\lambda + p_1(p_2 + q_2) - 2q_1^2](\lambda - p_2 + q_2) = 0$$

from it we can get

$$\lambda_1 = p_2 - q_2, \quad \lambda_2 + \lambda_3 = p_1 + p_2 + p_3, \quad \lambda_2\lambda_3 = p_1(p_2 + q_2) - 2q_1^2$$

if all the eigenvalues are negative, we need

$$(i) \lambda_1 < 0, \quad (ii) \lambda_2 + \lambda_3 < 0, \quad (iii) \lambda_2\lambda_3 > 0. \quad (5.8)$$

From (5.8), one gets

$$\lambda_1 = \frac{g_2 - g_1}{g_1 + g_2}\mu + \frac{4g_1 + g_2}{(g_1 + g_2)(g_1 - g_2)^2}h^2 < 0$$

that is to say

$$\mu < \frac{2g_1 + g_2}{(g_2 - g_1)^2}h^2.$$

From (3), one obtains

$$\lambda_2\lambda_3 = \left[ \mu - \frac{g_1}{(g_2 - g_1)^2}h^2 \right] \left[ \mu - \frac{2g_1 + g_2}{(g_2 - g_1)^2}h^2 \right] > 0$$

but the mixed solution requires

$$\rho_2 = \rho_3 = \sqrt{\frac{\mu - g_1\rho_1^2}{g_1 + g_2}} > 0 \quad \text{and} \quad g_1 + g_2 > 0,$$

and the inequality is  $\mu > \frac{2g_1 + g_2}{(g_2 - g_1)^2}h^2$ . It conflicts each other, so the mixed structure Turing pattern is always unstable.

**Theorem 2.** The dynamic system (5.3) has four kinds of solution, the stability as follows:

- (i) The stationary solution is stable for  $\mu < \mu_2 = 0$  and unstable for  $\mu > \mu_2$ .
- (ii) Stripe patterns solution is stable for  $\mu > \mu_3 = h^2 \frac{g_1}{g_2 - g_1}$  and unstable for  $\mu > \mu_3$ .
- (iii) Hexagon patterns solution exists when  $\mu > \mu_1 = \frac{-h^2}{4(g_1+2g_2)}$ ; The solution  $\rho^+ = \frac{|h| + \sqrt{h^2 + 4(g_1+2g_2)\mu}}{2(g_1+2g_2)}$  is stable only for  $\mu < \mu_4 = \frac{2g_1+g_2}{(g_2-g_1)^2}h^2$ , and  $\rho^- = \frac{|h| - \sqrt{h^2 + 4(g_1+2g_2)\mu}}{2(g_1+2g_2)}$  is always unstable.
- (iv) The mixed state solution exists when  $g_2 > g_1$  and  $\mu > \mu_3 = g_1\rho_1^2$ , and is always unstable.

In this section, we give the different condition for different patterns by the linear stability analysis of the amplitude equation.

## 6. Secondary bifurcation of Turing pattern

NWS equation, regarded as the normal form of a symmetry breaking bifurcation leading to roll stripe pattern and allowing for modulation in both  $x$  and  $y$  directions, is derived on the basis of amplitude equation and perturbation. Now we perform a linear stability analysis for  $\sigma = \text{Re}(\lambda)$  at  $(\mu_c, k_c)$ , and obtain

$$\begin{aligned}\sigma(\mu, k) = \sigma(\mu_c, k_c) + \left. \frac{\partial \sigma}{\partial \mu} \right|_c (\mu - \mu_c) + \left. \frac{\partial \sigma}{\partial k} \right|_c (k - k_c) + \frac{1}{2} \left. \frac{\partial^2 \sigma}{\partial \mu^2} \right|_c (\mu - \mu_c)^2 \\ + \frac{1}{2} \left. \frac{\partial^2 \sigma}{\partial k^2} \right|_c (k - k_c)^2 + \left. \frac{\partial^2 \sigma}{\partial \mu \partial k} \right|_c (\mu - \mu_c)(k - k_c) + \dots\end{aligned}$$

where  $\sigma(\mu, k) = 0$ ,  $\frac{\partial \sigma}{\partial k} = 0$  when the system is at the critical value  $(\mu_c, k_c)$  can be further reduced to the following form:

$$\sigma(\mu, k) = \left. \frac{\partial \sigma}{\partial \mu} \right|_c (\mu - \mu_c) + \frac{1}{2} \left. \frac{\partial^2 \sigma}{\partial \mu^2} \right|_c (\mu - \mu_c)^2 + \frac{1}{2} \left. \frac{\partial^2 \sigma}{\partial k^2} \right|_c (k - k_c)^2 + \left. \frac{\partial^2 \sigma}{\partial \mu \partial k} \right|_c (\mu - \mu_c)(k - k_c) + \dots$$

As the system nears the critical point, we assume

- (i)  $\varepsilon \sim \mu - \mu_c$
- (ii)  $\sigma \sim \varepsilon$  on the basis of the Turing bifurcation definition
- (iii)  $(k - k_c)^2 \sim \sigma \sim \varepsilon$
- (iv)  $\delta k_x^2 \sim \delta k_y^4 \sim \varepsilon$ .

From above we can know the equation has the following form on the leading order  $\varepsilon$

$$\sigma(\mu, k) = \left. \frac{\partial \sigma}{\partial \mu} \right|_c (\mu - \mu_c) + \frac{1}{2} \left. \frac{\partial^2 \sigma}{\partial k^2} \right|_c (k - k_c)^2$$

where the first order is the growth rate of instability module and the second order is the linear part influenced by other module.

For simplification, in this section, we only analyze the NWS equation for stripe pattern. The critical wave vector and perturbation are  $\mathbf{k}_c = (k_c, 0)$  and  $\delta \mathbf{k} = (\delta k_x, \delta k_y)$  respectively.

By using the Taylor series expansion we can obtain the leading  $\varepsilon$  order

$$(k - k_c)^2 = \left( \delta k_x + \frac{\delta k_y^2}{2k_c} \right)^2$$

where  $k = \sqrt{(k_c + \delta k_x)^2 + \delta k_y^2}$ .

In Fourier space, we have the following correspondence

$$\delta k_x \leftrightarrow -i \frac{\partial}{\partial X}, \quad \delta k_y \leftrightarrow -i \frac{\partial}{\partial Y} \quad \text{and} \quad (k - k_c)^2 = \left( \delta k_x + \frac{\delta k_y^2}{2k_c} \right)^2 \leftrightarrow - \left( \frac{\partial}{\partial X} - \frac{i}{2k_c} \frac{\partial^2}{\partial Y^2} \right)^2.$$

So we can get the NWS equation as follows:

$$\tau_0 \frac{\partial Z}{\partial t} = \mu Z + \xi_0^2 \left( \frac{\partial}{\partial X} - \frac{i}{2k_c} \frac{\partial^2}{\partial Y^2} \right)^2 - g_1 |Z|^2 Z \quad (6.1)$$

where  $\mu \leftrightarrow \frac{\partial \sigma}{\partial \mu}(\mu - \mu_c)$  and  $\xi_0^2 = -\frac{1}{2} \left. \frac{\partial^2 \sigma}{\partial k^2} \right|_c$ .

Now we give the linear stability analysis of system (6.1) and we assume

$$c = c_0 + Ae^{i(\delta kx+k_c)} + \text{c.c.}$$

where  $\delta k$  is the perturbation and  $k_c$  is critical wave.

Substitute  $Z = Ae^{i\delta kx}$  into system (6.1) and obtain

$$\tau_0 \frac{\partial A}{\partial t} = (\mu - \xi_0^2 \delta k^2)A + 2i\delta k \xi_0^2 \left( \frac{\partial}{\partial X} - \frac{i\partial^2}{\partial Y^2} \right) A + \xi_0^2 \left( \frac{\partial}{\partial X} - \frac{i\partial^2}{\partial Y^2} \right)^2 A - g_1 |A|^2 A. \quad (6.2)$$

Then we add the perturbation  $\delta A = u + iv$  to the amplitude  $A$  and substitute it into (6.2), obtain

$$\begin{aligned} \frac{\partial u}{\partial t} &= \left( -2(\mu - \delta k^2 \xi_0^2) + \xi_0^2 \frac{\partial^2}{\partial x^2} + 2\xi_0^2 \delta k \xi_0^2 \frac{\partial^2}{\partial y^2} - \xi_0^2 \frac{\partial^4}{\partial y^4} \right) u - \left( 2\delta k \xi_0^2 - 2\xi_0^2 \frac{\partial^2}{\partial y^2} \right) \frac{\partial}{\partial x} v \\ \frac{\partial v}{\partial t} &= \left( 2\delta k \xi_0^2 - 2\xi_0^2 \frac{\partial^2}{\partial y^2} \right) \frac{\partial}{\partial x} u + \xi_0^2 \left( \frac{\partial^2}{\partial x^2} + 2\delta k \frac{\partial^2}{\partial y^2} - \frac{\partial^4}{\partial y^4} \right) v. \end{aligned} \quad (6.3)$$

The perturbation  $u, v$  have the following decomposition

$$\begin{aligned} u &= Ue^{st} \cos(px) \cos(qy) \\ u &= Ve^{st} \sin(px) \sin(qy) \end{aligned}$$

and obtain the characteristic equation of (6.2) as follows:

$$\begin{vmatrix} s + 2(\mu - \xi_0^2 \delta k^2) + (p^2 + q^4 + 2\delta k p^2) \xi_0^2 & p \xi_0^2 (2\delta k + 2q^2) \\ p \xi_0^2 (2\delta k + 2q^2) & s + p^2 + 2\delta k q^2 + q^4 \end{vmatrix} = 0.$$

Thereout obtain the dispersion relation

$$\begin{aligned} s^2 + 2((\mu - \xi_0^2 \delta k^2) + (p^2 + 2\delta k q^2 + q^4) \xi_0^2) s + (2(\mu - \xi_0^2 \delta k^2) \\ + \xi_0^2 p^2 + 2\xi_0^2 \delta k q^2 + \xi_0^2 q^4)(p^2 + 2\delta k q^2 + q^4) \xi_0^2 - p^2 (2\delta k + 2q^2)^2 \xi_0^4 = 0 \end{aligned}$$

and it has two real roots as follows:

$$s_{\pm} = -[(\mu - \xi_0^2 \delta k^2) + (p^2 + 2\delta k q^2 + q^4) \xi_0^2] \pm \sqrt{(\mu - \xi_0^2 \delta k^2)^2 + p^2 \xi_0^4 (2\delta k + 2q^2)^2} \quad (6.4)$$

where a root  $s_-$  is always negative. Thereout the necessary condition of the stripe pattern instability is  $s_+ > 0$ . Obviously, the value  $s_+$  depends on the perturbation vector  $(p, q)$ .

We firstly assume  $q = 0$  and obtain from system (6.4)

$$s^2 + 2((\mu - \xi_0^2 \delta k^2) + p^2 \xi_0^2) s + (2(\mu - 3\xi_0^2 \delta k^2) + \xi_0^2 p^2) p^2 \xi_0^2 = 0.$$

As a result of  $s_- < 0$ , the instability condition is

$$s_- s_+ = [2(\mu - 3\xi_0^2 \delta k^2) + p^2] p^2 \leq 0.$$

The Eckhaus instability may occur when  $|\delta k| \geq \frac{\sqrt{3\mu}}{3\xi_0^2}$ . In virtue of  $s_+ = 0$  when  $p = 0$ , the critical perturbation is  $p \rightarrow 0$ . So the system has a long wave modulation  $p \rightarrow 0$ , which the magnitude increases as time when the stripe pattern of system lost stability.

Then assuming  $p = 0$  and obtain from system (6.4)

$$s^2 + 2((\mu - \xi_0^2 \delta k^2) + (2\delta k q^2 + q^4) \xi_0^2) s + (2(\mu - \xi_0^2 \delta k^2) + 2\xi_0^2 \delta k q^2 + \xi_0^2 q^4)(2\delta k q^2 + q^4) \xi_0^2 = 0$$

and easily get

$$s_+ = -q^2 (q^2 + 2\delta k x \xi_0^2).$$

The zigzag instability may occur when  $|\delta k| \leq -q^2$ . In virtue of  $s_+ = 0$  when  $q = 0$ , the zigzag instability is also longwave instability.

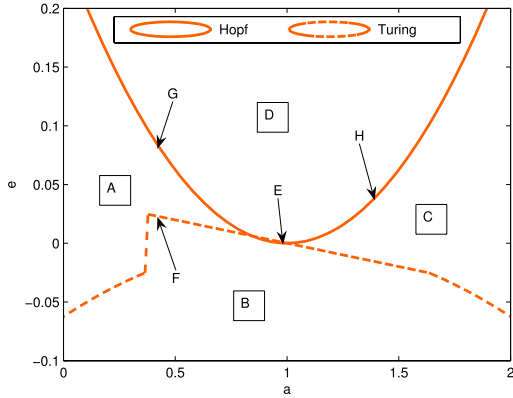


**Fig. 1.** Bifurcation diagram.

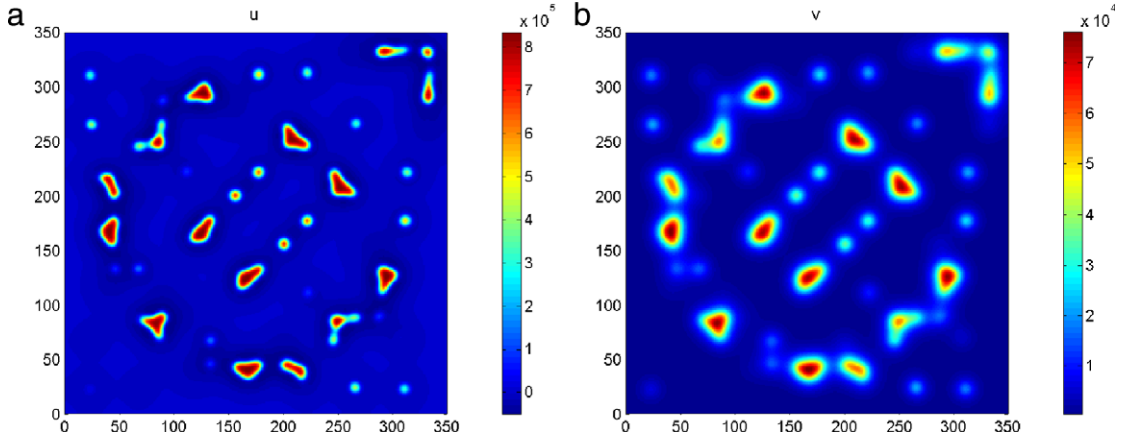


**Fig. 2.** In the domain A, two-dimensional approximate concentration  $u, v$  at  $T = 50$ , initial perturbation:  $\sin(XY)$  and  $\cos(XY)$  respectively. Parameter values are respectively  $a = 0.2$ ,  $e = 0.1$ .

The investigation of secondary bifurcation of Turing pattern by the linear stability analysis of NWS equation will derive the condition of the longwave instability based on the amplitude equation.

## 7. Numerical analysis

The system is simulated numerically in a  $350 \times 350$  two-dimensional square lattice. All our numerical simulations employ the zero-flux boundary conditions. We set time step and space step as 0.02 and 1, and select coefficients of diffusion  $(D_1, D_2) = (1, 4)$ , we choose parameters  $b = \frac{(a-1)^2}{4}$ . The domain above Turing and Hopf bifurcation lines is the region of the steady state (D). Both Turing and Hopf instability may occur when  $e$  decreases. For the low values of  $e$ , the Hopf bifurcation always precedes the Turing bifurcation. From Fig. 2 we can know the Turing bifurcation occurs firstly. In the pure Hopf instability domain, the system firstly becomes bulk oscillation, and then evolves into phase waves.

The bifurcation diagram is shown in Fig. 1. The bifurcation lines divide the bifurcation space into four domains (A, B, C, D) and (E, F, G, H) corresponds to different dots on the curve. In domain D, the system lies in the steady state. Domain A and C represent the regions of pure Turing and pure Hopf instabilities, respectively. In domain D, two bifurcations interact. In addition, F, G, H are on the line, and the E is an intersection. In our simulations, Figs. 2–4 show Turing instability near the critical condition, stable graph is observed in Fig. 5 in which red and bright colors are related to stable concentrations, respectively. With the distance to Turing bifurcation increased, patterns become unstable, and then convert to graph (Fig. 3). Fig. 4 undergoes the Eckhaus instability, resulting in labyrinthine graph. In addition we can find the different patterns formation under some conditions in Figs. 5–9 which mean that we can control the pattern formation, and further know the biological mechanism in it. In addition, some patterns of  $v$  are ignored which is similar to  $u$ .

In Fig. 10, Turing instability will occur when  $h(k^2) < 0$  or  $Re(\lambda) > 0$ , and zero is the critical value. There is coexistence of spot and stripe pattern in Fig. 11, more complicated patterns in Figs. 12–13 and spotted pattern in Fig. 14. After Eckhaus instability, the pattern wave of system increases or decreases, and zigzag instability, the stripes are not parallel, but form local zigzag patterns, such as Fig. 15(b), Fig. 16(b).

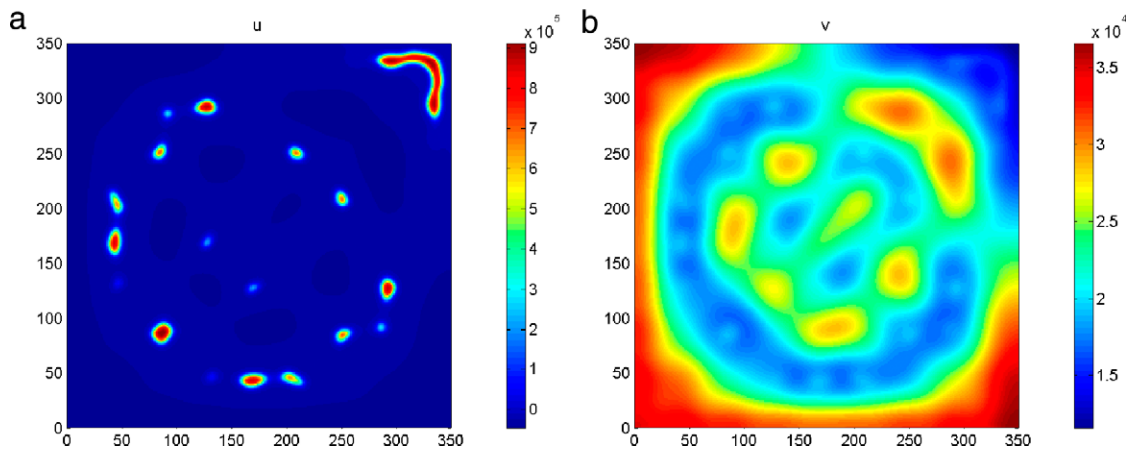


**Fig. 3.** In the domain  $B$ , two-dimensional approximate concentration  $u, v$  at  $T = 50$ , initial perturbation:  $\sin(XY)$  and  $\cos(XY)$  respectively. Parameter values are respectively  $a = 0.4$ ,  $e = 0.01$ .

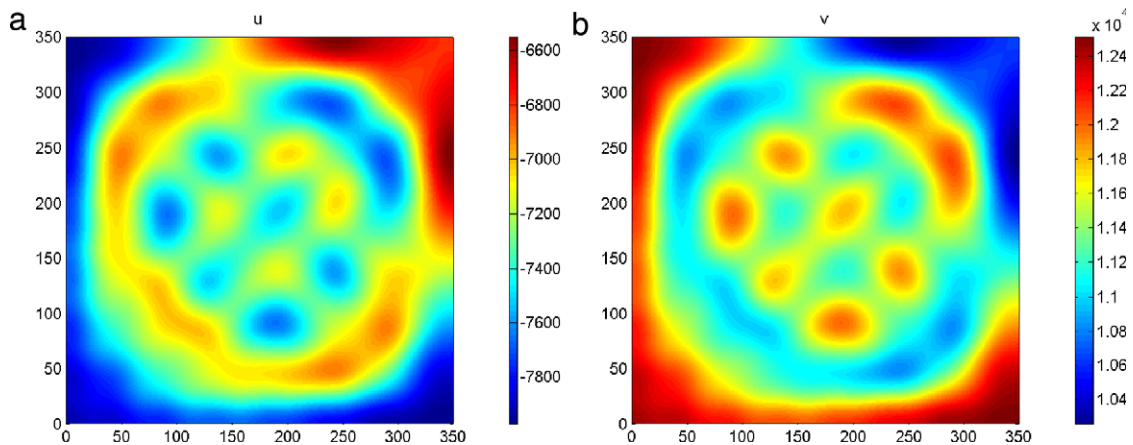


**Fig. 4.** In the domain  $C$ , two-dimensional approximate concentration  $u, v$  at  $T = 50$ , initial perturbation:  $\sin(XY)$  and  $\cos(XY)$  respectively. Parameter values are respectively  $a = 1.8$ ,  $e = 0.1$ .

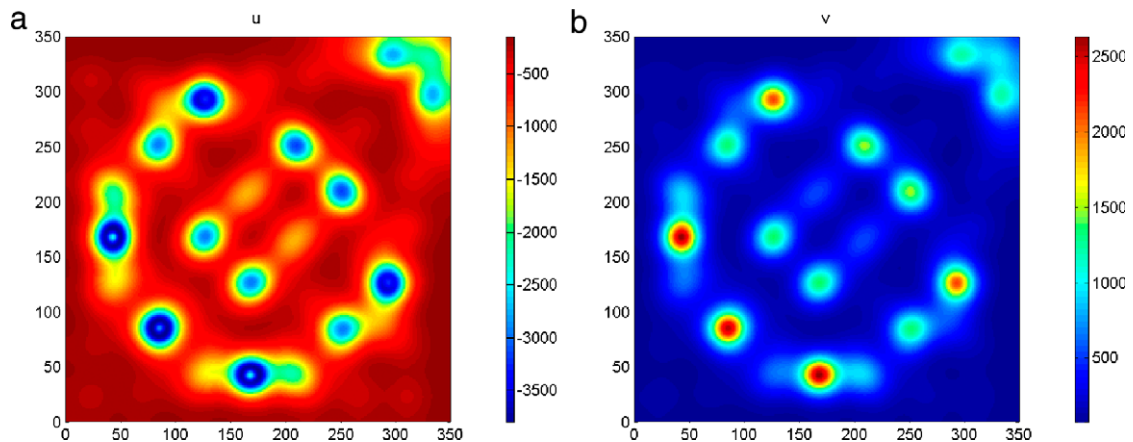


**Fig. 5.** In the domain  $D$ , two-dimensional approximate concentration  $u, v$  at  $T = 50$ , initial perturbation:  $\sin(XY)$  and  $\cos(XY)$  respectively. Parameter values are respectively  $a = 0.6$ ,  $e = 0.15$ . (For interpretation of the references to color in this figure legend, the reader is referred to the web version of this article.)

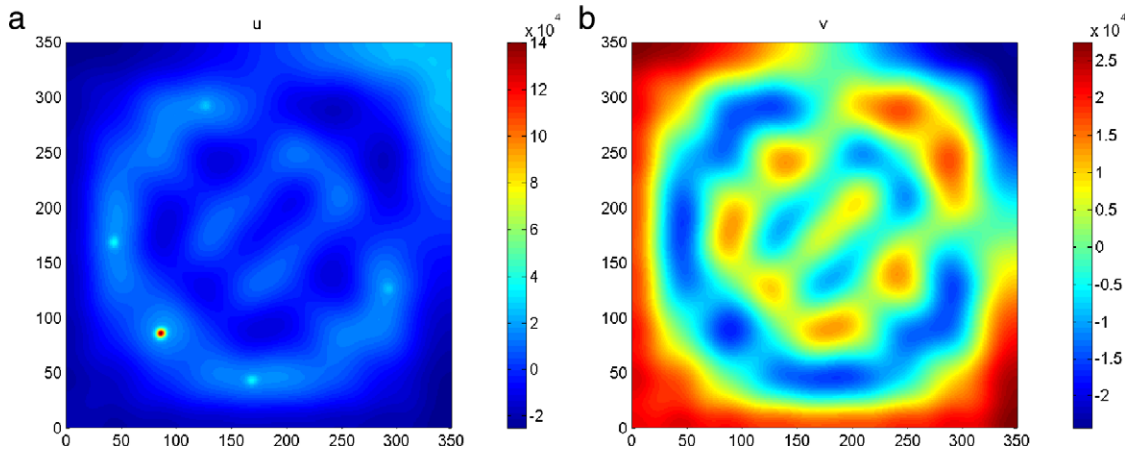


**Fig. 6.** At  $E$ , two-dimensional approximate concentration  $u, v$  at  $T = 50$ , initial perturbation:  $\sin(XY)$  and  $\cos(XY)$  respectively. Parameter values are respectively  $a = 1$ ,  $e = 0$ .

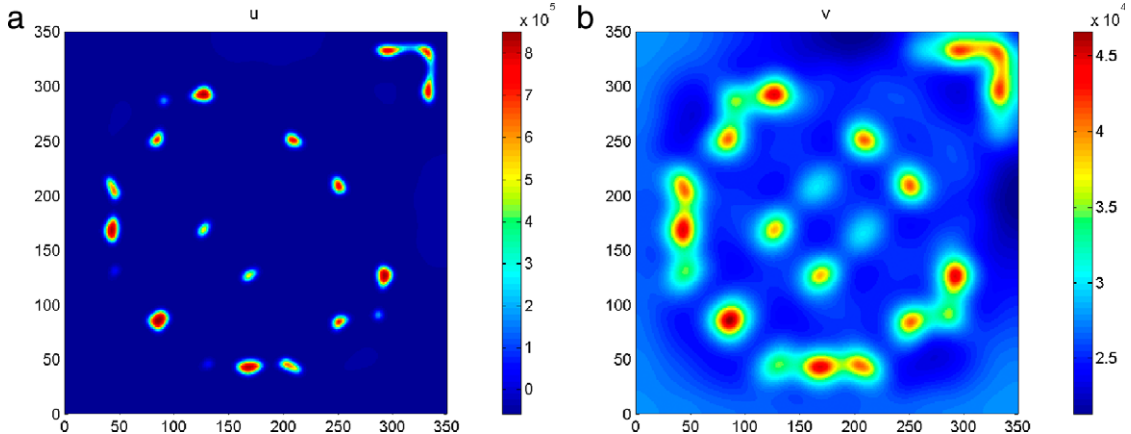


**Fig. 7.** At  $F$ , two-dimensional approximate concentration  $u, v$  at  $T = 50$ , initial perturbation:  $\sin(XY)$  and  $\cos(XY)$  respectively. Parameter values are respectively  $a = 0.4$ ,  $e = 0.0225$ .

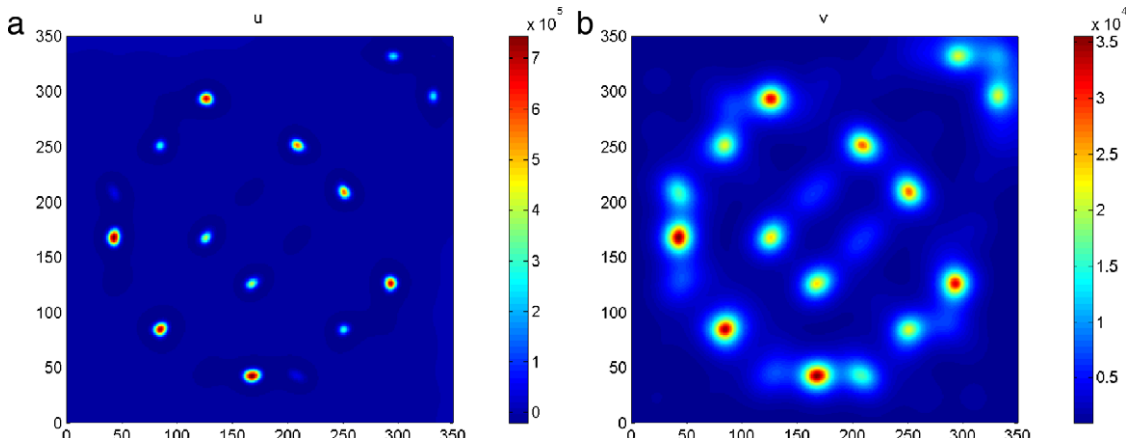


**Fig. 8.** At  $G$ , two-dimensional approximate concentration  $u, v$  at  $T = 50$ , initial perturbation:  $\sin(XY)$  and  $\cos(XY)$  respectively. Parameter values are respectively  $a = 0.4$ ,  $e = 0.09$ .

## 8. Conclusions

In this paper, we have carried out a detailed numerical investigation of generic Turing system and examined the effects of parameter for pattern formation and the interaction between Hopf bifurcation line and Turing bifurcation line. From

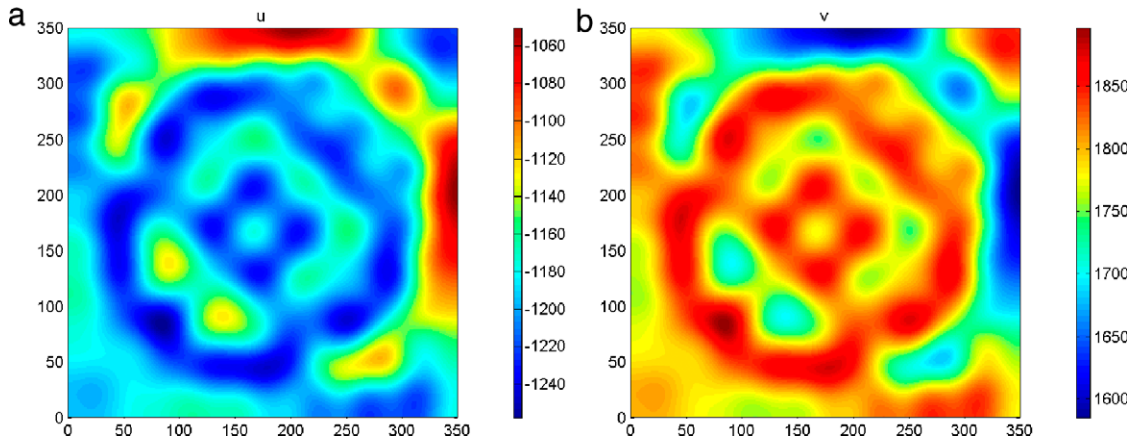


**Fig. 9.** At  $H$ , two-dimensional approximate concentration  $u, v$  at  $T = 50$ , initial perturbation:  $\sin(XY)$  and  $\cos(XY)$  respectively. Parameter values are respectively  $a = 1.6$ ,  $e = 0.09$ .

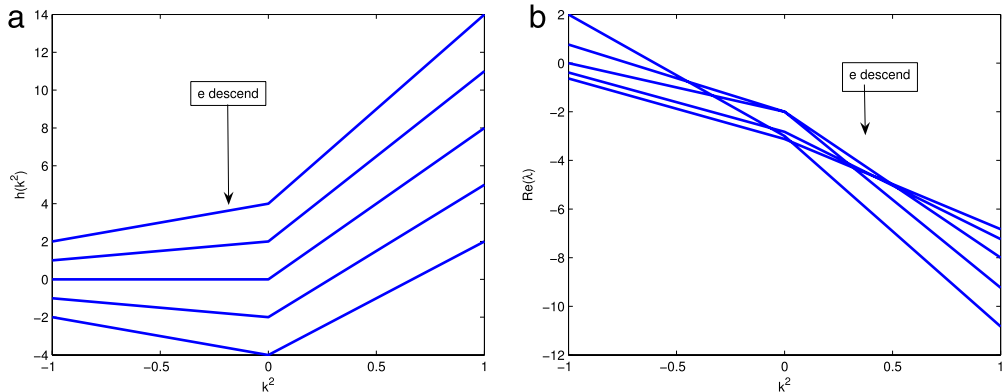


**Fig. 10.** (a) Plot of  $h(k^2)$  for typical kinetics, as the parameter  $e$  increases,  $h(k^2)$  becomes negative for a finite range, in which Turing instability when  $a = 3$ . (b) Plot of the largest of the eigenvalues  $Re(\lambda)$ , there is a range of wave numbers which are linearly unstable when  $a = 3$ .

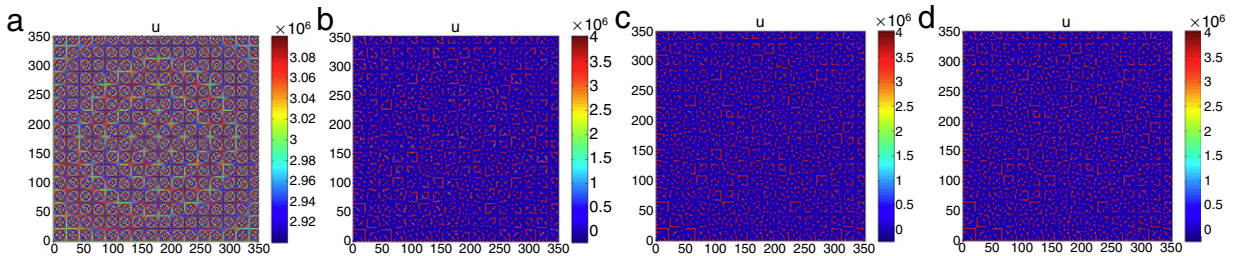


**Fig. 11.** There is coexistence of spotted and stripe patterns when  $\mu \in (\mu_3, \mu_4)$ , and figures (a-d, e-h) are respectively at time 0, 10, 80, 100. Parameter values and initial perturbation respectively:  $a = 5$ ,  $e = 5$ ,  $0.1 \sin(xy)$ .

numerical simulations, we have obtained spatiotemporal pattern in two-dimension space. Mechanism of these pattern is pure Turing, Hopf, wave instability and interaction between them. In addition, the model exists orderly spatiotemporal pattern when system is far away from equilibrium.

In [37], it gives us a way how to understand biological pattern formation. To compare the spatial dynamics for different parameter, we give the spatial pattern when the parameter values inside or outside of the domain of Turing space, the patterns above show that the distribution and interact of ion density and potential are caused by diffusion. The shade of color represents the variable of morphogens which means the concentration of ion in organism. We can control the pattern behavior through the variable of parameters. In this same way, we can control the distribution of ion, and further cure some diseases caused by the conduction of electrical impulses along a nerve fiber.

In final, we use a way (Taylor expansion) to derive the amplitude equation about the reaction–diffusion system which have fraction in the reaction item including variables, and prove it reasonable in the process.

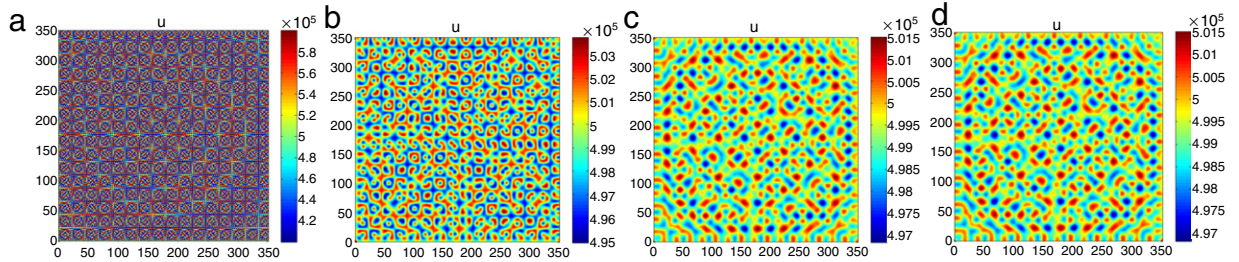


**Fig. 12.** The stripe pattern will occupy the whole space when  $\mu > \mu_4$ . However some stripe patterns connect with each other and cause the emergence of spotted pattern which is shown in Fig. 5. Figures (a-d, e-h) are respectively at time 0, 10, 500, 1000. Parameter values and initial perturbation respectively:  $a = 0$ ,  $e = 1$ ,  $0.1 \sin(xy)$ .

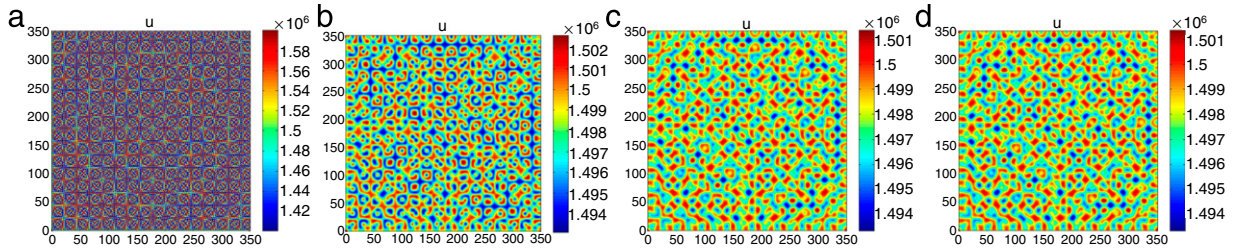


**Fig. 13.** We can find the coexistence of spotted and stripe patterns. Figures (a-d, e-h) are respectively at time 0, 10, 80, 100. Parameter values and initial perturbation respectively:  $a = 2$ ,  $e = 1$ ,  $0.1 \sin(xy)$ .

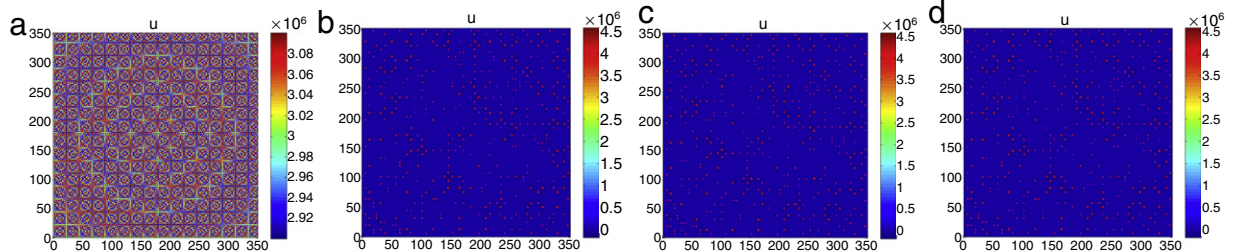


**Fig. 14.** The spotted patterns prevail over the two-dimensional space when  $\mu_1 < \mu < \mu_2$ . Figures (a-d, e-h) are respectively at time 0, 10, 80, 100. Parameter values and initial perturbation respectively:  $a = 5$ ,  $e = 1$ ,  $0.1 \sin(xy)$ .

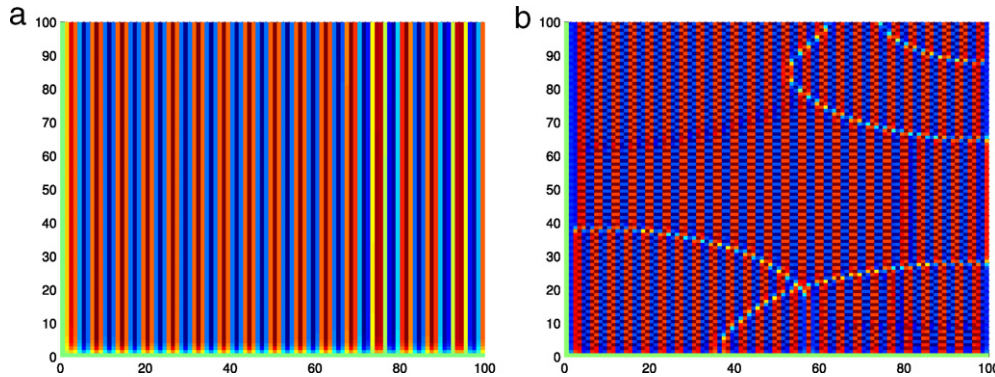


**Fig. 15.** (a) Is stable stripe pattern, (b) zigzag instability at  $T = 50$ , initial perturbation:  $\delta k = 1$  and  $\delta k = -0.1$  respectively. Parameter values are respectively  $a = 4$ ,  $e = 1$ .

## 9. Conflict of interests

The authors declare that there is no conflict of interests.

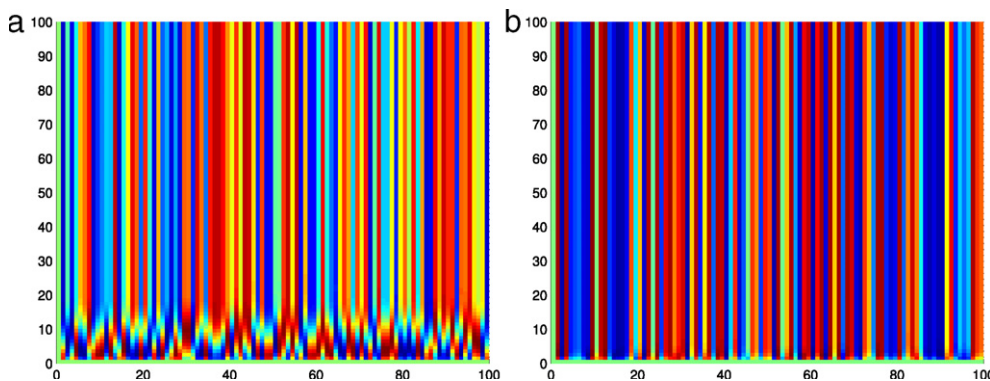


**Fig. 16.** (a) Is stable stripe pattern. (b) Eckhaus instability at  $T = 50$ , initial perturbation:  $\delta k = -1$  and  $\delta k = -1.5$  respectively. Parameter values are respectively  $a = 4$ ,  $e = 1$ .

## Acknowledgments

The authors are very indebted to the comments of reviewers. This work is supported by National Natural Science Foundation of China (11272277), Innovation Scientists and Technicians Troop Construction Projects of Henan Province (134100510013), Innovative Research Team in University of Henan Province (13IRTSTHN019) and International Cultivation of Henan Advanced Talents (201419). Dr. Jianwei Shen is indebted to Prof. Zhilin Qu for visiting the UCLA Cardiac Computation Lab in USA.

## References

- [1] A.H. Abbassian, H. Fallah, M.R. Razvan, Symmetric bursting behaviors in the generalized FitzHugh–Nagumo model, *Biol. Cybernet.* 107 (2013) 465–476.
- [2] M. Ringqvist, On dynamical behaviour of FitzHugh–Nagumo systems, *Res. Rep. Math.* (2006).
- [3] R. FitzHugh, Impulses and physiological states in theoretical models of nerve membrane, *Biophys. J.* 1 (6) (1961) 445–466.
- [4] A. Yazdan, G. Mehrdad, M. Ghasem, Pattern formation of the FitzHugh–Nagumo model: cellular automata approach, *Iran. I. Chem. Eng.* 30 (1) (2011) 135–142.
- [5] A. Panfilov, P. Hogeweg, Spiral breakup in a modified FitzHugh–Nagumo model, *Phys. Lett. A* 176 (1993) 295–299.
- [6] M.D. Angelis, P. Renno, On the Fitzhugh–Nagumo model, *Quant. Biol.* 1202 (5783) (2012) 1–8.
- [7] A. Malevanets, R. Kapral, Microscopic model for FitzHugh–Nagumo dynamics, *Phys. Rev. E* 55 (5) (1997) 5657–5670.
- [8] A. Dikansky, FitzHugh–Nagumo equation in a nonhomogeneous medium, *Discrete Contin. Dyn. Syst.* 2005 (2005) 216–224.
- [9] R. Torala, C. Masoller, R. Mirasso, et al., Characterization of the anticipated synchronization regime in the coupled FitzHugh–Nagumo model for neurons, *Physica A* 325 (2003) 192–198.
- [10] Y. Wu, P. Wang, et al., Turing patterns in a reaction–diffusion system, *Commun. Theor. Phys.* 45 (4) (2006) 761–764.
- [11] I. Lee, U.I. Cho, Pattern formations with turing and hopf oscillating pattern, *Bull. Korean Chem. Soc.* 21 (12) (2000) 1213–1216.
- [12] B. Pena, C. Perez, Stability of turing patterns in the Brusselator model, *Phys. Rev. E* 64 (2001) 056213.
- [13] H. Sayama, A.M. Marcus, D.E. Aguiar, et al., Interplay between turing pattern formation and domain coarsening in spatially extended population models, *Forma* 18 (2003) 19–36.
- [14] P.K. Maini, T.E. Woolley, R.E. Baker, et al., Turing's model for biological pattern formation and the robustness problem, *Interface Focus* 2 (2012) 487–496.
- [15] H. Kitano, Biological robustness, *Nat. Rev. Genet.* 5 (2004) 826–837.
- [16] A. Turing, The chemical basis of morphogenesis, *Trans. R. Soc. B* 237 (1952) 37–72.
- [17] Bard, Lauder, How well does Turing's theory of morphogenesis work, *J. Theor. Biol.* 45 (1974) 501–531.
- [18] S.M. Cohen, J. Brennecke, A. Stark, Denoising feedback loops by thresholding—a new role for microRNAs, *Genes Dev.* 20 (2006) 2769–2772.
- [19] Shigeru Kondo, Reaction–diffusion model as a framework for understanding biological pattern formation, *Science* 329 (1616) (2010) 1615–1632.
- [20] Q. Zheng, J. Shen, Dynamics and pattern formation in a cancer network with diffusion, *Commun. Nonlinear Sci. Numer. Simul.* 27 (2015) 93–109.
- [21] Q. Zheng, J. Shen, Turing instability in a gene network with cross-diffusion, *Nonlinear Dynam.* 78 (2014) 1301–1310.
- [22] X. Chen, J. Shen, H. Zhou, Attractor for a reaction–diffusion system modeling cancer network, *Abstr. Appl. Anal.* 2014 (2014) 420386.
- [23] H. Liu, W. Wang, The amplitude equations of an epidemic model, *Sci. Technol. Eng.* 10 (2010) 1929–1933.
- [24] A.K. Dutt, Amplitude equation for a diffusion–reaction system: The reversible Selkov model, *AIP Adv.* 2 (2012) 1–24.
- [25] G.H. Gunaratne, Q. Ouyang, H.L. Swinney, Pattern formation in the presence of symmetries, *Phys. Rev. E* 50 (1994) 2802–2820.
- [26] B. Pena, C. Perez-Garcia, Stability of turing patterns in the Brusselator model, *Phys. Rev. E* 64 (5) (2001) 9.
- [27] G. Sun, L. Li, Pattern dynamics in a spatial predator–prey system with Allee effect, *Abstr. Appl. Anal.* 2013 (2013) 1–12.
- [28] Q. Ouyang, Introduction to Nonlinear Science and Pattern Dynamics, Peking University Press, 2010.
- [29] Catalina Mayol, Raúl Toral, R.M. Claudio, Derivation of amplitude equations for nonlinear oscillators subject to arbitrary forcing, *Phys. Rev. E* 69 (6) (2004).
- [30] J. Murray, Mathematical Biology: I. An Introduction, in: Interdisciplinary Applied Mathematics, Springer, 2007.
- [31] Y. Kuramoto, Chemical Oscillations, Waves and Turbulence, Dover Publications, 2003.
- [32] M. Cross, H. Greenside, Pattern Formation and Dynamics in Nonequilibrium Systems, Cambridge University Press, 2009.
- [33] H. Yizhaq, Population dynamics study segregation as a nonlinear phenomenon, Ben-Gurion University of the Negev, Beer-Sheva, 2001.
- [34] Z. Song, C.Y. Ko, M. Nivala, J. Weiss, Z. Qu, Calcium-voltage coupling in the genesis of early and delayed afterdepolarizations in cardiac myocytes, *Biophys. J.* 108 (2015) 1908–1921.
- [35] Y. Chan, W. Tsai, Z. Song, et al., Acute reversal of phospholamban inhibition facilitates the rhythmic whole-cell propagating calcium waves in isolated ventricular myocytes, *J. Mol. Cell. Cardiol.* 80 (2015) 126–135.
- [36] M. Nivala, Z. Song, J. Weiss, Z. Qu, T-tubule disruption promotes calcium alternans in failing ventricular myocytes: Mechanistic insights from computational modeling, *J. Mol. Cell. Cardiol.* 79 (2015) 32–41.
- [37] T. Winfree, Varieties of spiral wave behavior: An experimentalist's approach to the theory of excitable media, *AIP Adv.* 1 (3) (1991) 304–334.